Manuscript accepted for publication in: Ogata et al., (eds). Submarine landslides: *Subaqueous Mass Transport Deposits from Outcrops to Seismic Profiles.* AGU Books

An Atlas of Mass-Transport Deposits in Lakes

Sammartini, M.[1]; Moernaut, J.[1]; Anselmetti, F.S.[2]; Hilbe, M.[2]; Lindhorst, K.[3]; Praet, N.[4]; Strasser, M[1].

[1] Institute of Geology, University of Innsbruck, Austria.

[2] Institute of Geological Sciences and Oeschger Centre for Climate Change Research, University of Bern, Switzerland.

[3] Institute of Geoscience, University of Kiel, Germany.

[4] Renard Centre of Marine Geology, Ghent University, Belgium.

Corresponding author: Michael Strasser (michael.strasser@uibk.ac.at)

Key Points:

- Bibliographic research on sublacustrine landslide-related studies and their distribution worldwide.
- Variabilities and commonalities of lacustrine Mass-Transport Deposits resulting from various mass-movement processes.
- Examples of vertical succession of intercalated Mass-Transport Deposits in lacustrine basin-fill sequences

Abstract

Mass-transport deposits (MTD) and related turbidites are common features in lacustrine environments and are intercalated within uniform lacustrine background sedimentation. Evidence of MTDs has been described worldwide in many lakes of different origin. They have been reported to result from various types of mass-movement processes, which can affect the subaquatic slopes but also the shoreline and basin.

Based on bibliographic research on sublacustrine landslide-related studies, we identified four different types of mass movements that occur independently from the type of lake, but differ in source area, type of failure initiation, transport mechanism and resulting MTDs. These are: (1) lateral slope landslides, (2) margin collapse, (3) delta collapses and (4) rockfalls. This study aims to illustrate variabilities and commonalities of lacustrine MTDs resulting from these four different mass-movement processes by presenting type examples of published multi-method investigations on lacustrine MTDs. Furthermore, this study provides a perspective on the wide range of applications of MTD research in lakes, due to their well-constrained boundaries, smaller size, continuity in sedimentation and the possibility to be surveyed on a complete basin-wide scale.

1 Introduction

Similar to advanced geophysical imaging, geotechnical testing and geological sampling of mass-transport deposits (MTD) and slope sequences in the oceanic realm, the understanding of subaquatic mass-movement processes has also advanced through numerous investigations in lakes (e.g. Chapron et al., 1999; Girardclos et al., 2007; Moernaut et al., 2017; Moernaut & De Batist, 2011; Schnellmann et al., 2002; Strasser & Anselmetti, 2008; Wiemer et al., 2015). Such limnogeological, process-oriented research on causes and consequences of mass movements in lakes have revealed that general characteristics of MTDs, as well as their underlying transport and initiation processes (e.g. slope preconditioning and landslide-triggering factors) are often comparable to those described in the classical submarine landslides literature (Hampton et al., 1996; Lamarche et al., 2016; Locat & Lee, 2002; Masson et al., 2006; Talling et al., 2015, and references therein). Given that lakes have well-constrained boundary conditions, smaller sizes and offer the possibility to be investigated on a complete basin-wide scale, studying mass movements in lacustrine environments offers a series of advantages that make lake studies vital to improve our knowledge on marine processes as well. In particular, hydroacoustic surveying in lakes typically uses higher frequencies and takes place in shallower water depths, leading to a higher signal-to-noise ratio and higher vertical resolution for bathymetric and subsurface structures than in many marine campaigns. Subbottom profiling in lakes often uses 3.5 kHz seismic sources, which result in a theoretical decimeter-scale vertical resolution. Furthermore, smaller water depths in lakes results in smaller spatial footprints of the geophysical signal and thus higher horizontal resolution. Due to the smaller scale of landslide features and – in many cases – limited sediment thickness overlying the bedrock, conventional coring from mobile platforms at comparably low logistical costs often reaches down to critical depths, crossing gliding surfaces. This allows a complete sampling and characterization of mass-transport deposits and the (intact) stratigraphic sequences adjacent to subaqueous slope failures.

Bibliographic research using key-word searches (in English) and citation analyses in different online research platforms, such as Web of Science, Google Scholar, and Research Gate, provides evidence of mass movements described in 172 lakes worldwide (Fig. 1 and supplementary data Table 1 with a complete list of all literature compiled in supplementary online file S-1). This compilation may not be complete, because some MTD descriptions in various lake publications have likely been missed due to differences in terminology and due to the fact that domestic scientific literature, in respective languages, has not been considered. Nevertheless, this compilation shows that mass movements occur in all types of lakes of different origins, such as glacigenic lakes (119 descriptions), tectonic lakes (23 descriptions), crater lakes (11 descriptions), dammed lakes (11 descriptions), karstic lakes (5 descriptions), meteorite impact lakes (2 descriptions), and fluvial lakes (1 description) (supplementary data Table 1).

Among all surveyed literature, 38 publications present a comprehensive, sublacustrine-landslide-related study that maps and characterizes at least one or more MTD in detail within the investigated lake. Other studies typically focus on other themes (e.g. paleoclimate or paleoenvironment) but describe or infer MTDs in either core or reflection seismic data. Above-mentioned distribution of MTD occurrences and lake types is certainly biased by the fact that various studies have different investigation foci and methodological approaches. Thus, the bibliographic data set cannot be statistically analyzed for process-based interpretations. However, we will start to categorize different generic types of mass movements in lakes, independently of the type of lakes in which they occur. In the following, we distinguish four main mass-movement types, based on their source areas, mode of failure initiation, transport mechanism and resulting MTD.

1) Lateral slope landslides occur on non-deltaic sublacustrine slopes characterized by hemipelagic draping sedimentation, and consist in a translational or rotational movement of coherent lake-internal sediments along a distinct basal shear surface. The lateral slope landslides are usually facilitated by the presence of a weak layer and triggered by external mechanisms, such as an earthquake or anthropogenic loading along the shoreline (e.g. Beigt et al., 2016; Lowag et al., 2012; Normandeau et al., 2016; Schnellmann et al., 2002; Simonneau et al., 2013).

2) Margin collapses are typically larger in extent and show complex, multi-stage failures, which affect the entire sublacustrine slope and (possibly) the shore. These, usually deep-seated failures, are controlled by local tectonic structures crosscutting lake morphology and are able to remobilize a great amount of different sediments and rocks (e.g. Chassiot et al., 2016; Gardner et al., 2000; Lindhorst et al., 2015).

3) Delta collapses are subaquatic slope failures on prograding river delta fans, beyond the gravitational sediment transport processes related to hydro-dynamics and sediment flux of the river itself. Depending on size and volume they show various failure modes initiated by either an external mechanism, such as an earthquake or a rockfall (e.g. Kremer et al., 2015; Praet et al., 2017; Van Daele et al., 2015), or they can occur spontaneously due to high sedimentation loading (Girardclos et al., 2007; Hilbe & Anselmetti, 2014, Vogel et al., 2015).

4) Rockfalls refer to a vertical or near-vertical fall of blocks and/or fragments of rocks from a very steep rock cliff. They can have both subaquatic and subaerial origin, the latter is common

in lakes in mountainous settings with steep rock cliffs surrounding the lake's shoreline (Bozzano et al., 2009; Karlin et al., 2004; Schnellmann et al., 2006).

All these mechanisms of failure can evolve downslope in sediment density flows, which can further be distinguished by their sediment concentration, nature and size of clasts, and flow rheology into debris flows or turbidity currents (Ito, 2008; Talling, 2013; Talling et al., 2015) resulting in various different types of deposits. However, this study of MTDs in lakes mainly presents geophysical data that cannot distinguish between these various flow types. Thus, adopting Dott´s classification (Dott, 1963), we refer to MTDs as all types of mass-movement deposits with the exception for deposits generated by turbidity currents combined with potentially related tsunami and seiche waves (Shanmugan, 2015, Schnellmann et al., 2005). For the latter we use the term turbidite, which indicates water-entrained and/or resuspended sediment transported in a turbulent flow that can cover the terminal depocentre of lacustrine basins with a typical ponding geometry. Whenever these units appear as mappable, homogenous to transparent seismic facies in reflection data, we refer to them as megaturbidites (according to the initial description by Bouma, 1987, and definition in lakes by Schnellmann et al., 2006).

This chapter presents MTDs and their cogenetic turbidites resulting from the 4 above-mentioned types of mass movements in lakes. We will present selected examples of published lacustrine MTD studies, reviewing and describing their characteristic features as observed in the different limnogeological datasets, and briefly discuss their underlying generic processes, also with respect to other global examples. This aims at (i) illustrating the variability and similarities of lacustrine MTDs resulting from different mass-movement processes, and (ii) providing views and perspectives of the wide range of fundamental to applied science applications of MTD research in lakes and beyond.

Figure 1 (see next page). Results of bibliographic research of MTDs in lakes. (a) World map with locations of the 172 lakes, with evidences of MTDs, found among all surveyed literature. Different symbols are used to mark lakes of different origin. The coloring of symbols is based on: the 7 lakes which provide case studies for this work are highlighted with red. Lakes referred to in this study are marked in yellow. All other lakes are marked in blue (see supplementary Table 1). (b) Zoom-in on central-southern Europe.

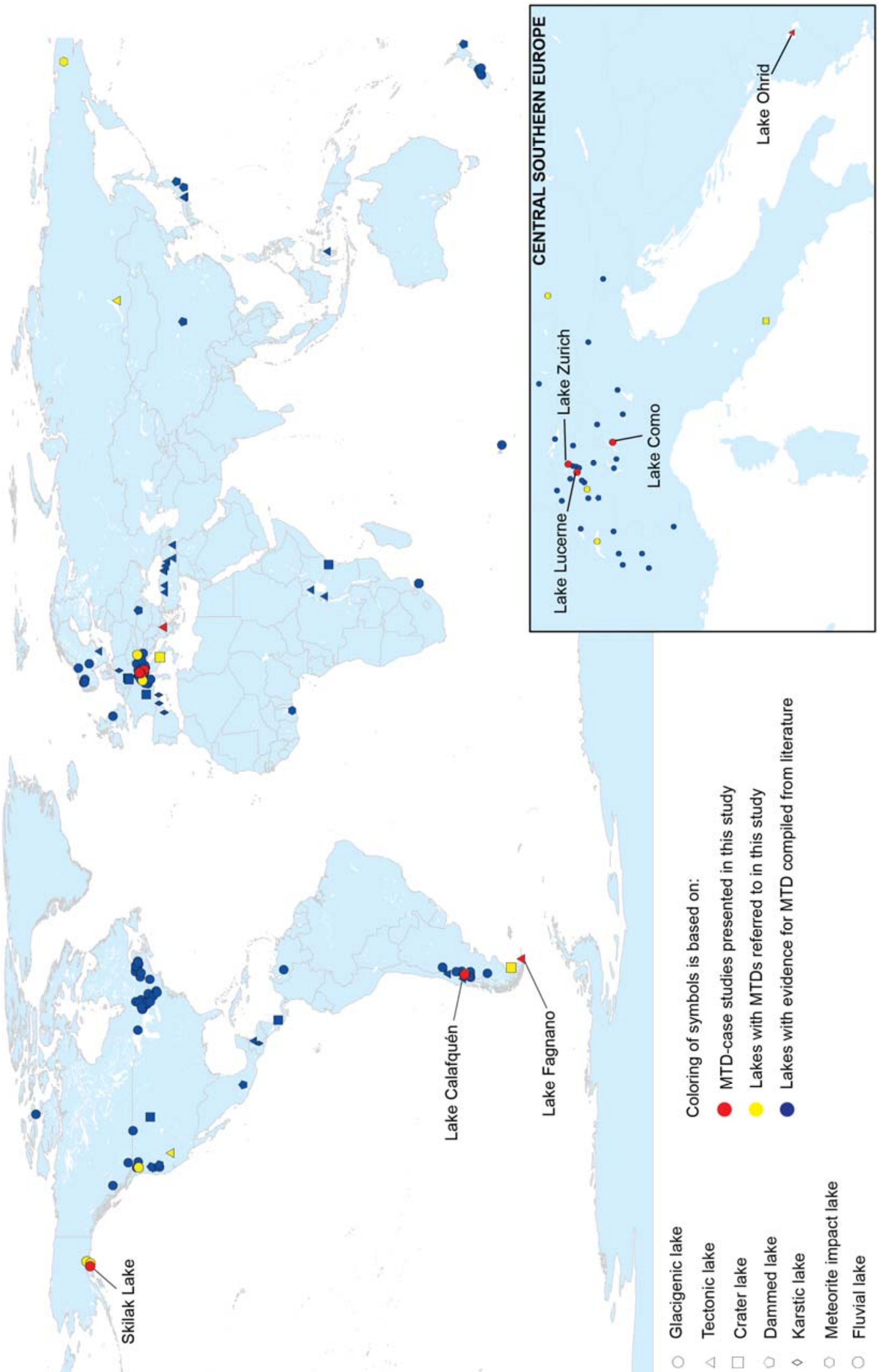

Skilak Lake
Lake Calafquén
Lake Fagnano
CENTRAL SOUTHERN EUROPE
Lake Lucerne
Lake Zurich
Lake Como
Lake Ohrid
Glacigenic lake
Tectonic lake
Crater lake
Dammed lake
Karstic lake
Meteorite impact lake
Fluvial lake
Coloring of symbols is based on:
MTD-case studies presented in this study
Lakes with MTDs referred to in this study
Lakes with evidence for MTD compiled from literature

131

2 Selected case studies of lacustrine MTDs resulting from different mass-movement processes

2.1 MTDs generated from lateral slope landslides

As selected case study, we present the neighboring Horgen and Oberrieden slides in Lake Zurich, Switzerland (Fig. 2), compiled after the original studies by Kelts & Hsu (1980), Strasser et al. (2013) and Strupler et al. (2017; 2018a). Perialpine Lake Zurich (47°15´ N; 8°41´ E; 135m deep) is located in northern Switzerland and occupies a glacially over-deepened trough. The southern slope of the central part of the main basin shows evidence of several subaqueous lateral slope landslides, which generated MTDs and turbidites that can be traced within the central basin (Strasser & Anselmetti, 2008). The 1875 AD Horgen slide and the 1918 AD Oberrieden slide represent two prominent examples of translational slides, in which the lacustrine sedimentary drape covering the slope has failed along a basal surface of glacial deposits due to human activity in the near-shore area (Fig. 2a). Even if they are only 1 km apart, the two resulting MTDs show different frontal emplacement styles. They are classified (following the classification scheme by Frey-Martinez et al., 2006) as a frontally emergent landslide (1875 AD Horgen slide), and a frontally confined landslide (1918 AD Oberrieden slide) (Strupler, 2017). The difference lies in the ability of the sliding mass to ramp up from its basal shear surface and travel downslope over layers of undisturbed sediments.

The 1875 AD Horgen slide represents a multiple-phase event (Kelts & Hsu, 1980) and is characterized by an irregular erosional surface of 0.33 km^2, with terraces and gullies. The depositional zone starts at the base of the slope and expands towards the central basin for ~630 m. The presence of several blocks with dimensions up to 20 m, allows differentiating the MTD from the lake bottom in multibeam bathymetry data (Fig. 2b). In seismic data the MTD is characterized by a transparent-to-chaotic facies. The MTD reaches its maximum thickness, which is ~6.6 m, at the base of the slope. The deposit thins towards the basin until it appears as a wedge that pinches out within parallel-stratified undisturbed sediments. A frontal ramp structure in the proximal part of the frontally emergent landslide (highlighted with a black solid line in Fig. 2d) marks the point in which the landslide was able to ramp up from the original basal shear surface and move downslope over undisturbed sediments. Turbidite deposits, in the deep basin, have been described in sediment cores by Kelts & Hsu (1980). Their longitudinal distribution along the axis of the deep basin suggests that turbidity currents generated by the sliding events were deflected by the opposite steep slope.

The single-phase 1918 AD Oberrieden slide covers a translational area of 0.16 km^2, with a clear scarp and the presence of various gullies on the steepest slope. The depositional zone consists of a rough surface with radially-parallel frontal bulges (`a´ white arrow in Fig. 2c). The bulges occur at the toe of the deposit forming a ~250 m wide zone within the frontal compressional regime during MTD emplacement. Such frontally confined MTDs are not able to ramp up from the basal surface. Therefore they undergo a restricted downslope translation with consequent ploughing of downslope adjacent sediments. As result of the frontal thrusts, the toe area is protruding from the lake bottom by ~3.5 m. The MTD is visible in seismic data as a transparent to chaotic unit with a maximum thickness that is larger in the distal part of the landslide body, where it reaches ~15 m. This area shows frontal thrust structures, which separate blocks of tilted and or/folded sediment sections (Fig. 2e).

According to Moernaut and De Batist (2011), the frontal emplacement of a slide is mainly controlled by the height of the center of gravity, which is determined, in turn, by the relative height drop between headscarp and frontal ramp and subsurface depth of the basal shear surface (i.e. the initial thickness of the sliding mass). A big height drop and a shallow basal shear surface result in a greater landslide´s ability to ramp out and evolve in a frontally emergent landslide. Furthermore, frontally emergent landslides usually show a higher mobility of the sliding deposits that are free to move outwards for long distances. In agreement with Moernaut and De Batist (2011), the frontally emergent Horgen slide shows higher values of height drop and smaller values of initial thickness of the sliding mass, i.e. 130 and 4 m against 83 and 11.5 m of the Oberrieden confined landslide. The emergent Horgen Slide is also characterized by a higher runout distance (1180 vs. 865 m).

Evidence of mass movements occurred in draped lateral slopes and resulting in comparable MTDs with either frontally emergent or frontally confined emplacement processes, are found in lakes of different origin worldwide. For instance, Anselmetti et al. (2009), which investigated the crater lake of Laguna Potrok Aike in Argentina, highlighted the presence of eight event horizons, with mass-movements originated from the lateral slopes, in the last 8600 cal yr BP. These instability events were more frequent during periods of high sedimentation and lowering of the lake´s water level. Lateral slope instabilities occurred also in Lake Baikal, the oldest and deepest lake on Earth, as documented in seismic data by several lense-shaped bodies with chaotic seismic facies (Solovyeva et al. 2016). These MTDs are separated in time, indicating repeated instability events from the same slope, most likely related to activity of the tectonic movements in the Baikal rift system.
Sauerbrey et al. (2013) identified and classified different types of Quaternary MTDs in meteorite-impact Lake El´gygytgyn. About 16% of the total sediment thickness accumulated in this 3.6 Myrs old Siberian lake is composed of MTDs from lateral slope landslides, which took place along a weak sediment layer, mobilizing and disintegrating packages of lacustrine sediments overlying it.

Figure 2 (see next page). Lateral slope MTD case study, Lake Zurich (Switzerland). (a) Location of the 1875 AD Horgen and the 1918 AD Oberrieden landslides in Lake Zurich. Black arrows: slide scarps; dotted black lines: deposit area. (b) Multibeam bathymetry data of the 1875 AD Horgen MTD. The deposit area is highlighted by the presence of several blocks. (c) Multibeam bathymetry data of the 1918 AD Oberrieden MTD. Parallel frontal bulges (marked with `a´ white arrow) outline the deposit extension. 3.5 kHz seismic profiles along the frontally emergent Horgen MTD (d) and the frontally confined Oberrieden MTD (e). Blue line and dashed blue line mark respectively the top and the base of the deposits. Location of profiles in Fig. 2b-c. Figures modified after Strupler et al., 2017.

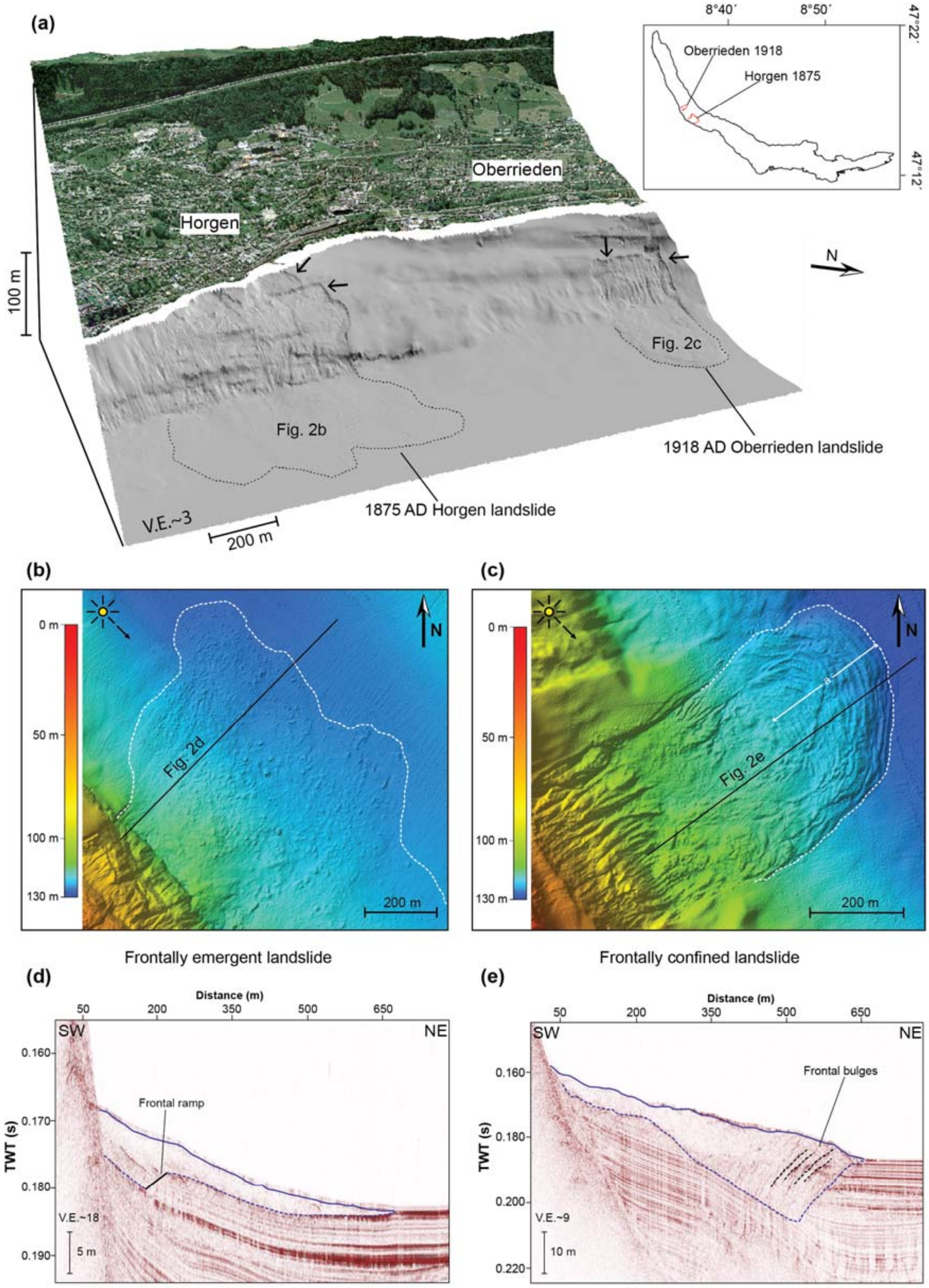
(a)
8°40′
8°50′
47°22′
47°12′
Oberrieden 1918
Horgen 1875
Oberrieden
Horgen
100 m
N
Fig. 2c
Fig. 2b
1918 AD Oberrieden landslide
1875 AD Horgen landslide
V.E.~3
200 m
(b)
(c)
0 m
50 m
100 m
130 m
N
Fig. 2d
Fig. 2e
200 m
Frontally emergent landslide
Frontally confined landslide
(d)
(e)
Distance (m)
50
200
350
500
650
SW
NE
TWT (s)
0.160
0.170
0.180
0.190
Frontal ramp
V.E.~18
5 m
0.200
0.220
Frontal bulges
V.E.~9
10 m

2.2 MTDs generated from margin collapses

Here we present the Udenisht slide complex (USC) in Lake Ohrid (Albania/Macedonia; Fig. 3) as an example of this complex mass-failure processes (Lindhorst et al., 2012; 2015; Wagner et al., 2012). Lake Ohrid (41°05′ N; 20°45′ E; maximum water depth 293 m) was formed between 3 and 5 Ma BP, representing one of the oldest lakes in Europe. It occupies approximately 360 km^2 of an active graben on the Balkan Peninsula. The USC is located in the southwestern part of the lake and represents the largest mass-wasting event found within the basin (Fig. 3a). It involved ~0,11 km3 of sediments of the southwestern margin, which travelled northeast for up to 10 km, covering almost 10% of the entire basin and reaching a maximum thickness of 50 m. Age estimations based on the thickness of the post-failure sediment drape suggest that the USC is most likely younger than 1500 years (Lindhorst et al., 2012).

The USC has been surveyed and described in detail with multibeam bathymetry, multichannel seismic and high resolution parasound data. Bathymetric data show that the failure zone is bounded by ~25-m high sidewalls. In the upper part, the zone is characterized by steep slope angles of up to 10° and in the lower part by an irregular topography (Fig. 3b-c), which is related to the presence of massive isolated blocks with dimensions up to 50 by 10 m. In 100 and 180 m of water depth, two parallel north-south striking morphological steps delineate tectonic faults (marked with black dashed lines in Fig. 3c), which likely played an important role in the instability occurrence and deposit distribution, as inferred from the geometrical relation between the USC sidewall and fault lineament. No clear head scarp is visible in the bathymetry data. This suggests a shallow (near-shore) initiation of the failure that involved the entire margin slope. The occurrence of two other slides, pockmarks structures and a prominent fault-related structure north of the USC slide area, hint towards a relationship between active tectonics, focused fluid flow and landslide initiation (Fig. 3b). The deposition area of the USC starts at ~150 m of water depth, where the slope angle is ~4°, and continues for up to 10 km into the deep basin, until it reaches an area with slope angle of less than 1.5°. The proximal part of the deposit is characterized by a hummocky top surface that stands out among the overall smooth topography. Moving towards the central basin, the top of the USC-MTD becomes smoother, and, therefore, hardly discernable from the general lake floor.

The multichannel seismic data show that the USC represents just the most recent of several MTDs that occurred in the same area (Fig. 3d). These deposits, which are visible as a chaotic-to-transparent seismic facies, intercalate conformable sub-parallel reflections. The northern sidewall of the USC landslide is visible as an abrupt 25-m high step in morphology. The thickness of the MTD increases gradually eastward towards the central basin, where bright spot amplitude anomalies, possibly related to fluid migration, are imaged (marked with blue circles in Fig. 3d).

A more detailed description of the USC features is obtained from 10-kHz parasound data (Fig. 3e). These data show that part of the transported mass has been trapped on the slope by several massive isolated blocks imaged on multibeam bathymetry. The MTD area is divided in three sections based on surface morphology, internal structure and thickness (Lindhorst et al., 2012). The upper section (I in Fig. 3e) shows a very rough topography and high-amplitude reflections within the deposit. The limited thickness of the deposit in this area allows identifying the base of the MTD, indicated by a high-amplitude seismic horizon (marked with a red dashed line in Fig. 3e). The middle section (II) corresponds with the main slide body. Here, the MTD is characterized by a maximum 50-m thick chaotic-to-transparent seismic facies with internal high-amplitude reflections. The high reflectivity of the lake floor prevents deeper penetration of the seismic signal, which is not reaching the base of the deposit. An abrupt decrease of the deposit thickness in combination with a frontal ramp structure within the deep basin separates section II from section III. The distal section (III) shows an irregular and discontinuous lake-floor reflection, indicating a high roughness of the top surface. Below and in front of the slide toe, parallel layers of undisturbed sediments are imaged. The collapse of the southwestern margin of Lake Ohrid occurred in at least two phases in a retrogressive pattern and it was most likely triggered by an earthquake (Lindhorst et al., 2012).

A big margin collapse has also been described in the tectonic Lake Tahoe, USA (Gardner et al., 2000) and relates, most likely, to the activity of the faults that border the lake basin, converging at a zone within McKinney Bay. Around ~60 ka BP (Smith et al., 2013), the entire north-western margin of the lake failed, generating a major mass movement that travelled towards the eastern margin. The failure brought to a change in the lake morphology, with the creation of the present-day McKinney Bay, a 12-km long embayment in the lake’s shoreline. The respective MTD is imaged in reflection seismic data as chaotic deposit with up to 40 m thickness across the deep basin, including big blocks up to 1000 m long and 80 m high, which are also prominently visible in bathymetric data.

Figure 3 (see next page). Margin collapse MTD case study, Lake Ohrid (Albania/Macedonia). (a) Location map of Lake Ohrid and margin collapse MTD. Blue and green boxes indicate positions of 3D perspective view and zoomed-in image shown as figures. (b) 3D perspective view of the southern area of Lake Ohrid. Red dashed line indicates the failure surface of the USC, yellow dashed line the MTD extension. Two smaller MTD, a fault and pockmark-like structures are marked north of the USC. (c) 3D image of the USC area with interpretation of the most prominent morphological features described in the text. (d) Multichannel seismic profile across the USC. Several MTDs, visible as chaotic-to-transparent facies among the normal sub-parallel reflections, are identified. The USC MTD is marked on top by a yellow line and at the base by a yellow dashed line. Older MTDs are marked with green lines. The sidewall of the margin collapse landslide and fluid migration-related features are marked in the figure. (e) Parasound profile cutting the USC failure surface and MTD with interpretation of the main instability-related features. The MTD is divided in three sections (I, II, III), described in the text. A dashed red line marks the base of the MTD. Figures modified after Lindhorst et al., 2012.

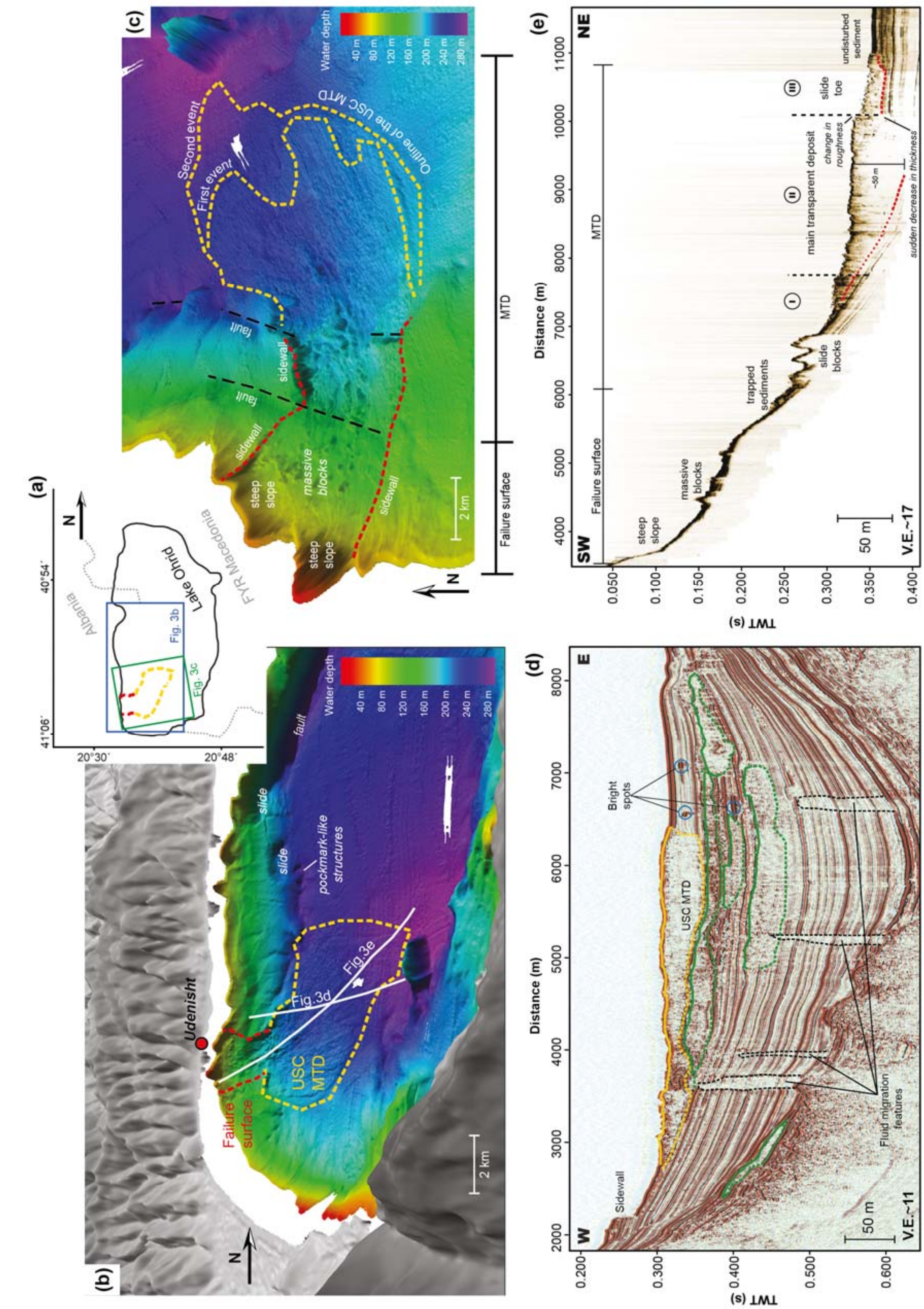
(a)
Lake Ohrid
Albania
FYR Macedonia
Fig. 3b
Fig. 3c
41°06'
40°54'
20°30'
20°48'
N
(b)
Udenisht
Failure surface
USC MTD
Fig.3d
Fig.3e
slide
slide
pockmark-like structures
fault
Water depth
40 m
80 m
120 m
160 m
200 m
240 m
280 m
2 km
N
(c)
Second event
First event
Outline of the USC MTD
fault
fault
sidewall
sidewall
sidewall
steep slope
steep slope
massive blocks
MTD
Failure surface
2 km
Water depth
N
(d)
W
E
Distance (m)
TWT (s)
Sidewall
USC MTD
Bright spots
Fluid migration features
50 m
V.E.~11
(e)
SW
NE
Distance (m)
TWT (s)
Failure surface
MTD
steep slope
massive blocks
trapped sediments
slide blocks
I
II
III
main transparent deposit
change in roughness
slide toe
undisturbed sediment
sudden decrease in thickness
~50 m
50 m
V.E.~17

2.3 MTDs generated from delta collapses

The Muota Delta collapse in Lake Lucerne (Switzerland) is presented to illustrate MTDs resulting from delta slope failures (Fig. 4) (Hilbe & Anselmetti, 2014; Siegenthaler & Sturm, 1991). This event occurred in AD 1687 and is historically documented as a 5 m high tsunami that took place during fair-weather and no-wind conditions (Billeter, 1923; Bünti, 1973; Dietrich, 1689). The Treib Basin and Lake Uri are two of the seven sub-basins of perialpine Lake Lucerne, a glacigenic lake in Central Switzerland (47°N, 8.4°E) (Fig. 4a). They have elongated shapes bounded by steep slopes and reach maximum depths of 123 m and 199 m for the Treib and Lake Uri basins, respectively. Both basins preserved evidence of the big subaqueous instability on the Muota delta in AD 1687 (Hilbe & Anselmetti, 2014).

The prograding delta of Muota River shows a complex morphological structure with lateral scarps and channels running from the central depositional fan to the deeper basins (Fig. 4b). In the western part, towards the Treib Basin, the slopes are characterized by low slope angles and smooth surfaces ("a" in Fig. 4b), whereas the eastern part shows steeper slopes with constant angles of about 20° -25° ("b" in Fig. 4b), which descend to Lake Uri. The headscarp of the AD 1687 delta collapse, which is not clearly detectable in this area, was most likely located within the currently active fan and is overprinted by the rapid deposition of post-event deltaic sediments (indicated with "c" black line in Fig. 4b). The Muota delta collapse evolved in two directions, forming MTDs with distinct characteristic features in both Treib Basin and Lake Uri (Hilbe & Anselmetti, 2014). The main part of the failed sediments descended towards Lake Uri, generating a MTD at the base of the slope and an associated turbidite, whereas westwards it induced deformation of the basin sediment of Treib Basin. Here, at the toe of Muota delta, a 300-m wide lobe structure extends for 800 m towards the basin and is delineated by an external bulge of 1-2 m height (marked with "d" in Fig. 4b). Smaller parallel bulges, protruding just a few decimeters, are present within the lobe ("e" in Fig. 4b). Towards the base of the slope they are replaced by a more hummocky topography.

The MTD in Lake Uri extends southward of the delta slope for 1.5 km, asymmetrically covering the entire basin in east-west direction, with thicknesses of 10 m in the east and 2-6 m in the west. In the northeastern part, the MTD shows a hummocky upper surface, with irregularities up to 30-m wide and 4-m high ("a" in Fig. 4c), which become less pronounced towards the southwest.

The seismic penetration is very low near the delta due to the presence of free gas in the sediments. The signal reaches 15 m depth in the central basin, revealing chaotic-to-transparent facies within the generally well-stratified sediments (Fig. 4d). Sediment cores show that the latter is mainly characterized by grey to brown muddy layers with intercalated thin turbidites, not resolvable in seismic data(Fig. 4e-A, core P5; Fig. 4e-C, core P7). On the seismic profiles, two major megaturbidites, with thicknesses of 1 and 1.5 m, are identified (MT1 and MT2 in Fig. 4d), both showing a ponding geometry. This basin-focused depositional pattern is most likely the result of seiches following the mass movement. These periodic oscillations of water level may move coarser sediments back and forth on the lake floor and keep the fine sediments in suspension for a longer period of time. This generates a focused and symmetrical deposition of sediments in the central basins (Beck, 2009; Hilbe & Anselmetti, 2014). In the cores, the corresponding turbidites usually have a sandy base, which creates a sharp contrast with the underlying undisturbed muddy layers (Fig. 4e-B, core P7).

The lower megaturbidite (MT2) is related to the Muota Delta collapse and is overlaying the associated MTD, which shows an irregular, southward-dipping top surface and ends with a 2-m high and 200-m wide tapering wedge that comprises layers of deformed laminated mud (Fig. 4e-D, core P6). Core P5 revealed in the uppermost meter of the MTD the presence of plants remains, mainly grass and some wood fragments, along with gravel and mud clasts (Fig. 4e-E, core P5), which are covering a sequence between almost homogeneous mud and mud-rich gravel with rounded pebbles (Fig. 4e-F, core P5). The total volume of the deposit is approximately 11 x 106 m^3 but a considerable part is not coming from the source area, as intact or weakly deformed blocks of sediments were entrained within the mass movement (Hilbe and Anselmetti, 2014).

Prograding delta fans are more susceptible to instability than non-deltaic draped lateral slopes, due to the high amount of clastic sediment input leading to oversteepening and possible development of pore-water overpressure. Therefore, mass movements in delta fans, with different size and triggering mechanisms, are common features in many lakes worldwide. For instance, a delta-slope failure was identified in Lake Quinault, USA, based on the presence of a MTD and megaturbidite in the deep basin, and can possibly be linked to the giant (M_w~9) AD 1700 Cascadia earthquake (Leithold et al., 2018). Megathrust earthquakes are also interpreted as a trigger for delta collapse-related MTDs occurring at correlative stratigraphic levels across three south-central Alaskan proglacial lakes (Praet et al., 2017). Delta and alluvial fan failure deposits, related to the AD 1964 Alaska Earthquake, represent 95% of the total landslide volume in Kenai Lake, 33-39% in Eklutna Lake and 15% in Skilak Lake. A spontaneous delta collapse occurred in spring AD 1996 in Lake Brienz (Switzerland). The event was detected by a series of events (i.e. seiches, turbidity increase and low oxygen concentrations in deep waters) and created a large megaturbidite deposit, which is covering the flat lake basin (Girardclos et al., 2007). In Lake Geneva, a large delta collapse in AD 523, resulting in a prominent MTD and megaturbidite deposit, was triggered by a subaerial rockfall loading and mobilizing the water-saturated delta plain (Kremer et al., 2015).

Figure 4 (see next page). Delta collapse MTD case study, Lake Lucerne (Switzerland). (a) Location of the Treib and Lake Uri basins in Lake Lucerne. Red and blue boxes indicate positions of detailed bathymetric maps shown as figures. (b) Multibeam bathymetric data of Muota delta and the easternmost part of Treib Basin. Features described in the text are labelled: `a´ slope with low slope angles and smooth surfaces; `b´ slope with steep angles; `c´ currently active fan; `d´ external bulge of collapse-related lobe; `e´ small parallel bulges within the deposit. (c) Multibeam bathymetric data of the northern part of Lake Uri showing a hummocky surface at the toe of the Muota delta (`a´). (d) 3.5 kHz seismic profile along the northern part of

Lake Uri, see Fig. 4c for location. The AD 1687 Muota delta collapse MTD is marked with blue line on top and blue dashed line at the base. The related megaturbidite and a younger megaturbidite are outlined (top: solid line; base: dotted line) and labelled (MT2 and MT1). Vertical black lines show the position of sediment core, and white boxes with black outline show the detailed location of images presented in Fig. 4e. (e) Photographs of split core surfaces showing typical lithologies from Lake Uri: (A) laminated muddy layers with turbidites; (B) sandy base of collapse-related megaturbidite (MT2); (C) laminated muddy layers with turbidites; (D) deformed laminated mud in frontal wedge of Muota delta collapse MTD; (E) accumulation of plants remains; (F) muddy gravel with rounded pebbles. Red and blue lateral lines indicate respectively turbidite layers and the sandy base of MT2. Figures modified after Hilbe and Anselmetti, 2014.

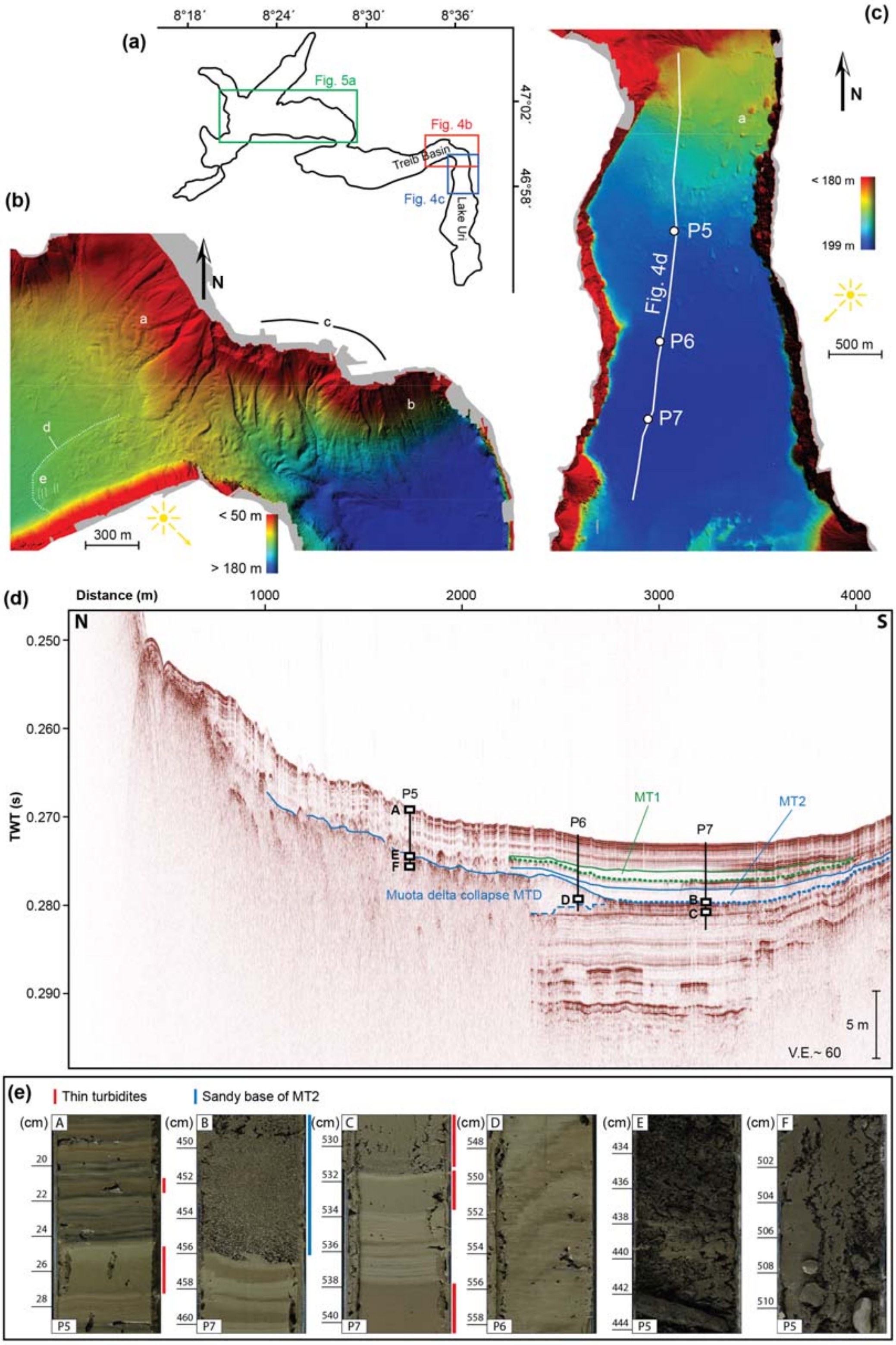

(a)
8°18´
8°24´
8°30´
8°36´
47°02´
46°58´
Fig. 5a
Fig. 4b
Fig. 4c
Treib Basin
Lake Uri
(b)
N
a
b
c
d
e
300 m
< 50 m
> 180 m
(c)
N
a
< 180 m
199 m
P5
P6
P7
Fig. 4d
500 m
(d)
Distance (m)
1000
2000
3000
4000
N
S
TWT (s)
0.250
0.260
0.270
0.280
0.290
MT1
MT2
Muota delta collapse MTD
5 m
V.E.~ 60
(e)
Thin turbidites
Sandy base of MT2
(cm)
A
B
C
D
E
F
P5
P7
P6

2.4 MTDs generated from rockfalls

Repeated rockfall activity from the steep cliff of Bürgenstock Mountain, on Lake Lucerne (Switzerland), offers a representative case study for MTDs related to this type of gravitational mass movement (Fig. 5) (Hilbe et al., 2011; Schnellmann et al., 2006). The Vitznau Basin is one of the three distal basins of Lake Lucerne, Central Switzerland (47°N, 8.4°E) and is located at the Alpine Front. The basin is surrounded to the south by the steep limestone cliffs of Bürgenstock Mountain, and to the north by the conglomerate slopes of Rigi Mountain, which show a more gentle topography. Rockfall deposits and rockfall-evolved MTDs are abundant in the Vitznau Basin, and they are present at the base of the slopes in the form of debris cones (Fig. 5a). These generally triangular-shaped deposits show hummocky, irregular topography and positive relief on bathymetric maps. The bathymetric data of the Vitznau Basin highlights the presence of a major event at the base of Rigi Mountain, as well as several repeated events at the toe of the Bürgenstock cliffs (Fig. 5a). In this area rockfalls originate from the steep slopes above lakeshores, as highlighted by the presence of subaerial scarps (Fig. 5b).

Schnellmann et al. (2006) report at least six rockfall events that occurred in the Bürgenstock cliff area during the last 12000 years, with the latest correlated to a strong regional earthquake in AD 1601. On the bathymetry data, this area shows two distinct rockfall cones, both characterized by hummocky surfaces with only large-scale irregularities (Fig. 5c). Small-scale irregularities, most likely associated with isolated blocks, which have been smoothed out by post failure sedimentation. The larger cone, located to the west, covers an area of approximately 0.2 km^2 and extends for 320 m north to the base of the slope. On seismic data, it appears as a chaotic seismic facies with some discontinuous high-amplitude reflections and an irregular upper surface (Fig. 5d). This irregular surface and the likely presence of isolated blocks lead to a low penetration of the seismic signal. At the foot of the rockfall cone, three MTDs are identified at different stratigraphic levels (marked with I, II and III in Fig. 5d). They are likely to be rockfall-evolved deposits and, therefore, their presence confirms a repeated rockfall activity in this area. These wedge-shaped units, of which the thickness is decreasing towards the basin, are characterized by a chaotic seismic facies with high-amplitude reflections. This common feature for rockfall-evolved deposits is most likely related to the presence of rock fragments in a muddy matrix, as shown in the core of Fig. 5e. The core in Fig. 5d represents the sedimentary succession through a rockfall-evolved deposit and highlight the presence of limestone fragments up to 5 cm within the deposit. The deposit overlies laminated layers of undeformed sediments and is, in turn, overlain by a 10-cm thick turbidite.

Rockfalls are common events in subaerial steep slopes and can generate water waves and secondary instabilities on the subaquatic slopes, leaving significant imprints in the lacustrine record. The AD 1960 Great Chilean Earthquake (M_w 9.5) triggered several rockfalls along the slopes bordering Lake Pellaifa. Several of these rockfalls surged into the lake leading to a reported tsunami and subsequent seiche, which resulted in the deposition of a 2-m thick megaturbidite in the deep basin (Van Daele et al., 2015). Daxer et al. (in press) reports the occurrence of repeated rockfall activity from the southern shore of Lake Mondsee (Austria), based on morphological evidence and seismic and core data. The infrequent but repeated rockfalls originated from a steep and weathered cliff, shaping the present-day morphology of the shore. Even if the volumes of these events are not comparable with the ones in Lake Lucerne, the instabilities have led to various sedimentological imprints in the near-shore area, as indicated by cores and seismic data. Rockfall deposits are the most frequent instability events in Lake Albano, Italy, as reported by Bozzano et al. (2009). All these deposits are related to combined subaerial-subaqueous instability events, as suggested by the presence of subaerial scarps along the shoreline and of subaquatic deposits, such as “block fields” and isolated blocks of up to 100 m^2 wide that are visible on the lake floor.

Figure 5 (see next page). Rockfall MTD case study, Lake Lucerne (Switzerland). (a) Bathymetric map of Chrüztrichter and Vitznau basins in Lake Lucerne with interpretation of the main observed morphologies, including rockfall cones. See Fig. 4a for location. Figure modified after Hilbe et al., 2011. (b) Aerial photograph of the steep slope of Bürgenstock Mountain. A dashed red line marks the rockfall scarp. Photograph by Bernd Nies. (c) Detailed bathymetric data of two rockfall cones, marked with white dashed line, at the toe of Bürgenstock Mountain (see Fig. 5a for location). (d) 3.5 kHz seismic profile across a major rockfall cone. At the foot of the rockfall cone, three rockfall-evolved MTDs are identified at different stratigraphic levels, suggesting a repeated rockfall activity from the Bürgenstock cliffs. See Fig. 5c for location. Figure modified after Schnellmann et al., 2006. (e) Example of sediment core through rockfall-evolved MTD and photograph of rock fragments. Figure modified after Schnellmann et al., 2006.

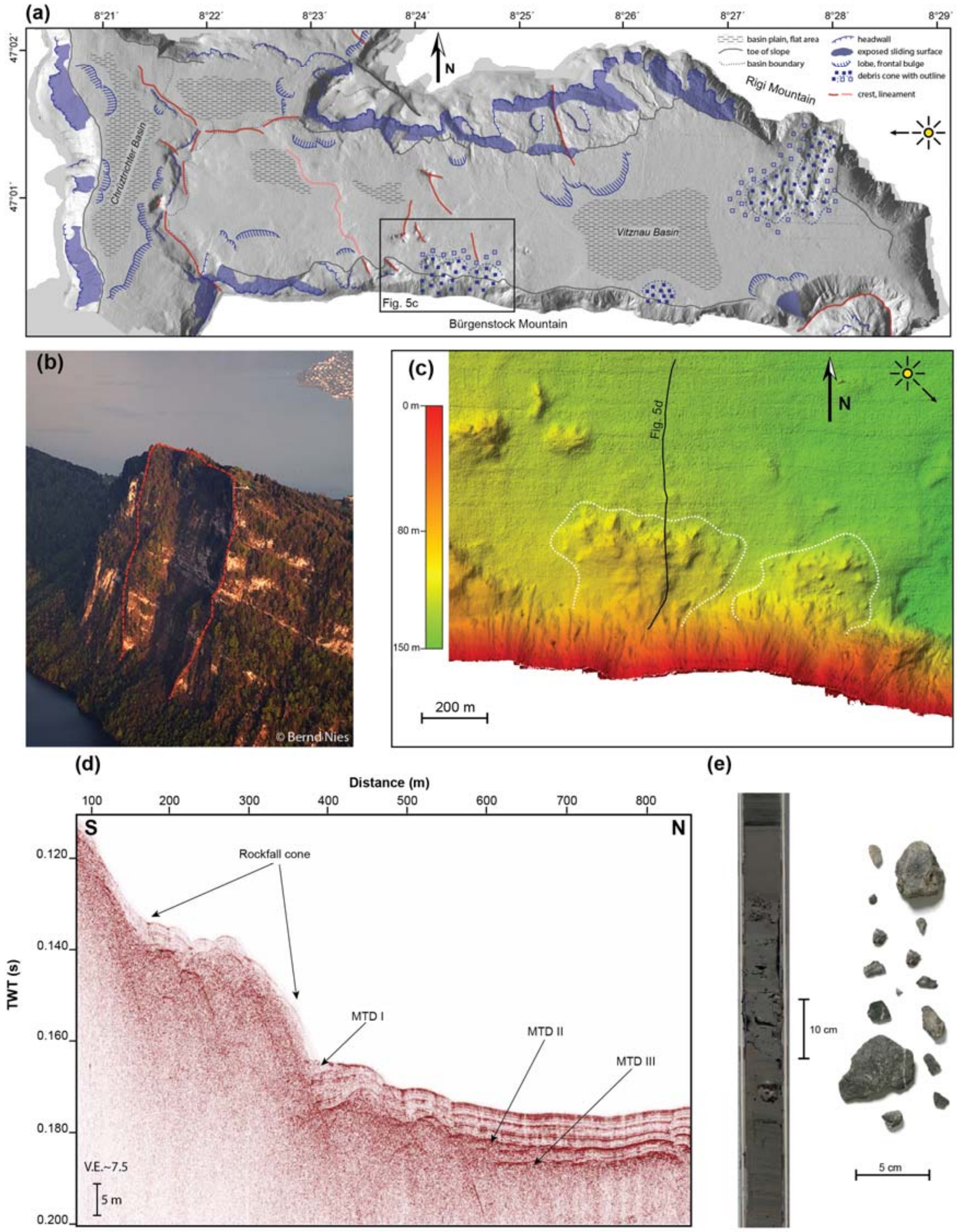

(a)
8°21´
8°22´
8°23´
8°24´
8°25´
8°26´
8°27´
8°28´
8°29´
47°02´
47°01´
N
basin plain, flat area
toe of slope
basin boundary
headwall
exposed sliding surface
lobe, frontal bulge
debris cone with outline
crest, lineament
Rigi Mountain
Chrüztrichter Basin
Vitznau Basin
Fig. 5c
Bürgenstock Mountain
(b)
© Bernd Nies
(c)
0 m
80 m
150 m
Fig. 5d
N
200 m
(d)
Distance (m)
100
200
300
400
500
600
700
800
S
N
0.120
0.140
0.160
0.180
0.200
TWT (s)
Rockfall cone
MTD I
MTD II
MTD III
V.E.~7.5
5 m
(e)
10 cm
5 cm

3 Vertical succession of intercalated MTDs in basin-fill sequences

As already mentioned in several of the examples presented above, MTDs originating from different types of instability are often intercalated within the lacustrine normal background sedimentation, representing a distinct MTD-stratigraphy. MTDs often appear to be deposited in a vertical succession, suggesting a repeated destabilization of the same slope area though time. In the sedimentary sequence, these deposits are generally separated by layers of undisturbed sediments, of which the thickness depends on the background sedimentation rate and on the frequency of mass movements.

In the following we will present 4 examples of vertical succession of intercalated MTDs visualized on 3.5 kHz pinger seismic data from four different lakes worldwide (Fig. 6). We briefly showcase how identification and dating of MTDs stratigraphy extends the historic event catalogue to prehistoric times, unraveling geological information about the long-term instability occurrence linked to either long-term preconditioning or short-term trigger factors as they may relate to past climate, environment and/or seismotectonic conditions.

Figure 6 (see next page). Examples of vertical succession of intercalated MTDs. MTDs are marked on top by solid line and at the base by dashed line. (a) 3.5 kHz seismic profile in Skilak Lake (Alaska). 7 event horizons are identified, each comprising coeval MTDs. The youngest event, in orange, corresponds to the AD 1964 (M_w 9.2) earthquake in Alaska. Figure modified after Praet et al., 2017. (b) 3.5 kHz seismic profile in Lake Como (Italy). Two prominent MTDs, labelled with `MTD1´and `MTD2´, and their related megaturbidites (top: solid line; base dotted line) are identified at the toe of Bellagio Plateau. Figure modified after Fanetti et al., 2008. (c) 3.5 kHz seismic profile in Lake Fagnano (Argentina/Chile). Several MTDs are identified at different stratigraphic levels. The asymmetry of the most prominent event, highlighted in light blue, leads to an inclined post-failure stratigraphy. Figure modified after Waldmann et al., 2011. (e) 3.5 kHz seismic profile in Lake Calafquén (Chile). Several frontally emergent MTDs are identified at the base of the slopes. The largest deposit, highlighted in green is the result of three simultaneous failures along different slopes. Above this horizon, fluid/sediment escape features, possibly related to earthquake-induced liquefaction and fluidization of buried MTD soft sediments, are marked. Figure modified after Moernaut et al., 2017.

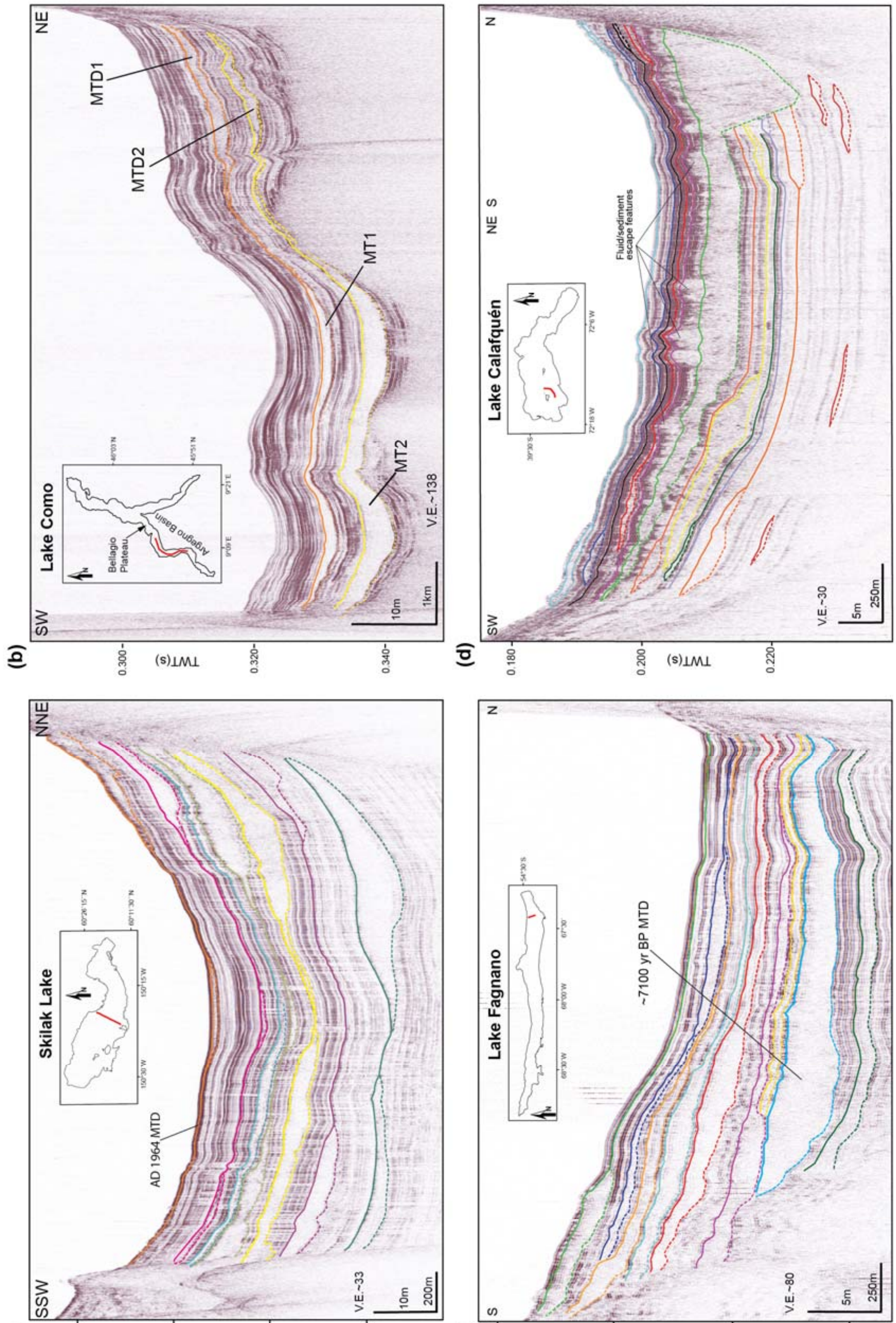
(a)
Skilak Lake
SSW
NNE
AD 1964 MTD
V.E.~33
10m
200m
TWT (s)
0.240
0.260
0.280
0.300
(b)
Lake Como
Bellagio Plateau
Argegno Basin
SW
NE
MTD1
MTD2
MT1
MT2
V.E.~138
10m
1km
TWT(s)
0.300
0.320
0.340
(c)
Lake Fagnano
S
N
~7100 yr BP MTD
V.E.~80
5m
250m
TWT(s)
0.240
0.250
0.260
0.270
(d)
Lake Calafquén
SW
NE S
N
Fluid/sediment escape features
V.E.~30
5m
250m
TWT(s)
0.180
0.200
0.220

3.1 Skilak Lake

Skilak Lake is a glacigenic lake on the Kenai Peninsula, in south-central Alaska (60°24′N; 150°20′W). The lake basin consists of two sub-basins: a deep proximal basin, with maximum depth of 194 m that gradually transitions into a shallower distal basin, which reaches 140 m depth. Based on seismic stratigraphic interpretations, Praet et al. (2017) map several MTDs intercalated between the uniform background sedimentation, as well as their related megaturbidites in the central part of the deep basin. Seven event horizons are identified, each of them comprising multiple coeval MTDs widespread over the lake basins (Figure 6a). Instabilities, which comprise mostly lateral slope landslides, occurred on both northern and southern slopes, as indicated by the stratigraphically-correlated MTDs at the base of the opposite slopes. These failures can also generate megaturbidites, which were deposited in the deepest part of the lake and which are characterized by the typical ponding geometry. Seismic data show that the northern MTDs are usually larger than the southern ones. This is interpreted as a consequence of the larger amount of sediments on the more gentle northern slopes, compared to the steeper southern ones. The youngest event (marked with orange lines) corresponds to the AD 1964 (M_w 9.2) earthquake in this area. This earthquake triggered a total of 23 mass movements in Skilak Lake with a total volume of 9.9 x 107 m^3. The related megaturbidite has an estimated total volume of 2.7 x 106 m^3. Synchronous failure of different lacustrine slopes hints at regional trigger mechanism, such as a strong earthquake. Thus, prehistoric stratigraphic levels with coeval landslides can be used to infer the occurrence of strong earthquakes (Praet et al., 2017).

3.2 Lake Como

Lake Como (46°10′N; 09°16′E) is located in the Italian Alps and has depths of up to 425 m. It has a glacial origin enhanced by tectonic preconditioning and therefore has a complex shape with three lake branches. The deepest part of the lake (Argegno Basin) is situated in the southwestern branch, which is separated from the other branches by a submerged plateau (Bellagio plateau). Two prominent MTDs and their associated megaturbidites are identified from reflection seismic data in the Argegno basin (Fig. 6b) (Fanetti et al., 2008). The two MTDs are located at the foot of the plateau at ~5m and ~8m subsurface depth. The basinward-(southward) thinning, wedge-shaped MTD bodies, with irregular and locally erosive basal and hummocky top surfaces, have similar chaotic-to-transparent reflectivity patterns, which is in clear contrast to the high-amplitude and continuous reflections of undisturbed sediments, above, between and below. The MTDs are the result of large slides that occurred on the steep slopes of the plateau. A morphological sill, which divides the upper and deepest part of the basin, defines the distal limits of the MTDs and most likely has played an important role in the evolution of the mass flows into turbidity currents. The correlative megaturbidites are prominently imaged as an acoustically-transparent seismic facies and sharp, high-amplitude upper and lower reflections between the horizontally-stratified background sediments. They show a ponding geometry onlapping on the basin edges and they extend over the entire basin length (~5 km), reaching maximum thicknesses of 1.5 m (MT1) and 3 m (MT2). As these megaturbidites are not yet cored, Fanetti et al. (2008), estimated the ages from near-surface radio-nuclide (Cs-137) dating and extrapolation of sedimentation rates and suggest that the events occurred in the 12th (MT1) and 6th centuries (MT2). Since there is historical evidence for a strong regional earthquake in the 12^{th} century, Fanetti et al., (2008) further speculated that the observed mass-movements in Lake Como could have triggered by seismic shaking of the sediment-overloaded steep slope of the Bellagio plateau.

3.3 Lake Fagnano

Lake Fagnano (54°32´S; 67°59´W) is located on the main island of Tierra del Fuego (Argentina/Chile), in a pull-apart basin that was further shaped by glaciers. It is divided in a western basin and a smaller eastern basin with maximum depths of 110 and 210 m, respectively. The seismic data in the eastern basin allow identifying several event horizons of synchronous MTDs and related megaturbidites within well-stratified sediments (Fig. 6c) (Waldmann et al., 2011). The chaotic seismic facies of MTDs are located at the base of the southern slope and are getting thinner toward the center of the basin. The MTDs generally have smooth upper surfaces, but show irregular bases, which are locally eroding and deforming the overridden basin sediments. In the deep basin, related megaturbidites are identified as seismically-transparent facies with ponding geometry. The most prominent event (in light blue in Fig. 6c), was dated ~7100 yr BP taking into consideration one regionally-documented tephra layer, radiocarbon ages and modeled sedimentation rates. This MTD is lens-shaped and fills the basin in an asymmetric way, leading to an inclined post-failure basin stratigraphy. This inclination is further enhanced by the repeated occurrence of mass-movements from the southern slope and is clearly preserved in the actual lake bottom morphology.

The simultaneous occurrence of different mass movements suggests an external trigger mechanism, most likely earthquakes along the active Magallanes-Fagnano transform fault, which were able to mobilize the sedimentary drape of the southern slope. The northern slope is too steep to permit sediment accumulation.

3.4 Lake Calafquén

Lake Calafquén (39°31´ S; 72°08´ W) is a glacigenic lake at the foot of the south-central sector of the Andes. It consists of a main large basin with depths up to 215 m, and a smaller basin to the south-west. The studied SW basin is characterized by numerous coeval MTDs at different stratigraphic layers (Fig. 6d). The MTDs are located at the base of the slopes and are classified as frontally emergent landslides, as shown by the presence of frontal ramps in the seismic data (Moernaut, 2010).

The largest deposit, highlighted in green (Fig. 6d), covers the entire southwestern basin and is the result of three simultaneous failures along different slope segments. The mass movement has deeply deformed the sediments at the base of the slope, which become therefore included in the chaotic-to-transparent facies of the deposit. Vertical acoustic wipe-outs and intercalated upward-concave zones of up to 80-m wide and 1.9-m thick with low-amplitude reflections are identified above the deposit and have been related to fluid migration activity. Moernaut et al. (2009) suggests that these features have been created by earthquake-induced liquefaction and fluidization of the soft sediments of the buried MTD, resulting in sediment extrusions at the contemporaneous lake bottom, forming sediment volcanoes.

The presence of multiple MTDs in all the stratigraphic event horizons suggests that the occurrence of instabilities is strictly related to the seismic activity of the area, which is dominated by the megathrust earthquake cycle of the Chilean subduction zone (Moernaut et al., 2014, 2017). The youngest event corresponds to the giant AD 1960 (M_w 9.5) earthquake, which generated instabilities along the steep flanks of the lake. It comprises seven MTDs located at the base of the slope and a 5-cm thick turbidite, which cannot be identified on seismic data, but which was confirmed by cores (Moernaut et al., 2017).

4 Discussion/Conclusion

Bibliographic research highlights that mass movements are common processes in all types of lacustrine environments and can be classified based on the source area, initiation and transport mechanisms, and resulting MTDs and megaturbidites. In particular, we focused on four different instability mechanisms and their related deposits. The reported examples highlight that in reflection seismic data, MTDs often show similar features, even when related to different mass movement processes. These common features include their geometries (wedge-shaped bodies), internal seismic facies (typically characterized by chaotic-to-transparent facies), the irregularity of the upper surface, and the presence of related megaturbidites towards the basin. Nevertheless, the use of multi-method investigations on lake-basin wide scales brings complementary information about the erosional and depositional area, allowing to differentiate between different mass-movement mechanisms.

In the last decades the study of sublacustrine instabilities became increasingly important in different research fields, e.g. paleoclimate, paleoseismology and natural hazard assessment. Due to their small size, well-constrained boundaries, and spatial and temporal continuity in sedimentation, lakes provide well-datable sedimentary archives of the past environmental and climatic changes of the lake and its surrounding. Furthermore, high-energy natural events, such as earthquakes, floods, shore and delta collapses have been shown to leave important fingerprints in the lacustrine sedimentation, allowing to extend the historic event catalogue to prehistoric times. Single MTDs with large correlative megaturbidites can be caused by e.g. spontaneous delta collapse, for which no external trigger is needed (e.g. Girardclos et al., 2007), while strong earthquakes have been proven to be able to generate synchronous basin-wide mass movements and resuspend large amounts of sediments (Schnellmann et al., 2002). The resulting coeval multiple MTDs and related megaturbidites form distinct and characteristic fingerprints of past earthquakes in the sedimentary record (Kremer et al., 2017, and Praet et al., 2017 and referenced therein). The identification and dating of these synchronous instability events allows reconstructing frequency and seismic mechanisms of paleo-earthquakes in the area (Doughty et al., 2014; Howarth et al., 2014). When the studied lake and geophysical imaging reveals vertical succession of intercalated MTDs, which can be cored to date the event horizons, the earthquake recurrence pattern can be analyzed. Furthermore, integration of these data with other data set allows for rough estimates of the magnitude of causing earthquake (Becker et al., 2005; Boës et al., 2010; Kremer et al., 2017; Lauterbach et al., 2012; Strasser et al., 2006, 2013). Thus, studies of historic and prehistoric instabilities and their deposits are essential for natural hazards assessment, which also includes slope-stability analysis and tsunami modeling (Lindhorst et al., 2014; Strasser et al., 2011; Strupler et al., 2017, 2018a, 2018b).

One key question in the current research of landslide is whether the lacustrine landslides can be scaled up to the much larger marine landslide. If lakes could be considered as small scale model of marine environment, the study of lacustrine mass movement would become even more significant, improving our understanding of marine instability events with the details and advantages of lacustrine investigations.

Acknowledgments

This work is supported by the European Training Network SLATE (Submarine Landslide and their impact on European continental margins), in the frame of the Marie-Skłodowska-Curie program.

The authors would like to thank Marc De Batist, Nicolas Waldmann and Sebastian Krastel for sharing their data and Bernd Nies for kindly allowing the use of his aerial photograph.

HIS Markit is acknowledged for their educational grant program providing the KINGDOM seismic interpretation software.

We thank editor Andrea Festa and two anonymous reviewers for handling and constructive comments on the manuscript.

References

Anselmetti, F. S., Ariztegui, D., De Batist, M., Catalina Gebhardt, A., Haberzettl, T., Niessen, F., ... & Zolitschka, B. (2009). Environmental history of southern Patagonia unravelled by the seismic stratigraphy of Laguna Potrok Aike. *Sedimentology*, *56*(4), 873-892.

Beck, C. (2009). Late Quaternary lacustrine paleo-seismic archives in north-western Alps: Examples of earthquake-origin assessment of sedimentary disturbances. *Earth-Science Reviews*, *96*(4), 327-344.

Becker, A., Ferry, M., Monecke, K., Schnellmann, M., & Giardini, D. (2005). Multiarchive paleoseismic record of late Pleistocene and Holocene strong earthquakes in Switzerland. *Tectonophysics*, *400*(1-4), 153-177.

Beigt, D., Villarosa, G., Gómez, E. A., & Manzoni, C. (2016). Subaqueous landslides at the distal basin of Lago Nahuel Huapi (Argentina): Towards a tsunami hazard evaluation in Northern Patagonian lakes. *Geomorphology*, *268*, 197-206.

Billeter, J. (1923). *Pfarrer Jakob Billeter von Aegeri und seine Chronik. Heimat-Klänge, Sonntags-Beilage zu den "Zuger Nachrichten"*. Jahrgang, 4, 28.

Boës, X., Moran, S. B., King, J., Cağatay, M. N., & Hubert-Ferrari, A. (2010). Records of large earthquakes in lake sediments along the North Anatolian Fault, Turkey. *Journal of Paleolimnology*, *43*(4), 901-920.

Bozzano, F., Mazzanti, P., Anzidei, M., Esposito, C., Floris, M., Fasani, G. B., & Esposito, A. (2009). Slope dynamics of Lake Albano (Rome, Italy): insights from high resolution bathymetry. *Earth Surface Processes and Landforms*, *34*(11), 1469-1486.

Bouma, A. H. (1987). Megaturbidite: an acceptable term?. *Geo-Marine Letters*, *7*(2), 63-67.

Bünti, J. L., & Wyrsch, J. (1973). *Chronik des Johann Laurentz Buenti, Landammann: 1661-1736*. Historischer Verein Nidwalden.

Chapron, E., Beck, C., Pourchet, M., & Deconinck, J. F. (1999). 1822 earthquake-triggered homogenite in Lake Le Bourget (NW Alps). *Terra Nova*, *11*(2-3), 86-92.

Chassiot, L., Chapron, E., Di Giovanni, C., Albéric, P., Lajeunesse, P., Lehours, A. C., & Meybeck, M. (2016). Extreme events in the sedimentary record of maar Lake Pavin: Implications for natural hazards assessment in the French Massif Central. *Quaternary Science Reviews*, *141*, 9-25.

Daxer, C., Moernaut, J., Taylor, T., Haas, J.N., & Strasser, M. (in press). Late glacial and Holocene sedimentary infill of Lake Mondsee (Eastern Alps, Austria) and historical rockfall activity revealed by reflection seismics and sediment-core analysis. *Austrian Journal of Earth Science* (in press). DOI:10.17738/ajes.20180.008.

Dietrich, J. (1689). *Diarium von P. Josep Dietrich von Einsiedeln (1645-1704).* Klosterarichiv Einsiedeln

Dott Jr, R. H. (1963). Dynamics of subaqueous gravity depositional processes. *AAPG Bulletin*, *47*(1), 104-128.

Doughty, M., Eyles, N., Eyles, C. H., Wallace, K., & Boyce, J. I. (2014). Lake sediments as natural seismographs: Earthquake-related deformations (seismites) in central Canadian lakes. Sedimentary Geology, 313, 45-67.

Fanetti, D., Anselmetti, F. S., Chapron, E., Sturm, M., & Vezzoli, L. (2008). Megaturbidite deposits in the Holocene basin fill of Lake Como (southern Alps, Italy). *Palaeogeography, Palaeoclimatology, Palaeoecology*, *259*(2-3), 323-340.

Frey-Martínez, J., Cartwright, J., & James, D. (2006). Frontally confined versus frontally emergent submarine landslides: a 3D seismic characterisation. Marine and Petroleum Geology, 23(5), 585-604.

Gardner, J. V., Mayer, L. A., & Hughs Clarke, J. E. (2000). Morphology and processes in lake Tahoe (California-Nevada). *Geological Society of America Bulletin*, *112*(5), 736-746.

Girardclos, S., Schmidt, O. T., Sturm, M., Ariztegui, D., Pugin, A., & Anselmetti, F. S. (2007). The 1996 AD delta collapse and large turbidite in Lake Brienz. *Marine Geology*, *241*(1-4), 137-154.

Hampton, M. A., Lee, H. J., & Locat, J. (1996). Submarine landslides. *Reviews of geophysics*, *34*(1), 33-59.

Hilbe, M., & Anselmetti, F. S. (2014). Signatures of slope failures and river-delta collapses in a perialpine lake (Lake Lucerne, Switzerland). *Sedimentology*, *61*(7), 1883-1907.

Hilbe, M., Anselmetti, F. S., Eilertsen, R. S., Hansen, L., & Wildi, W. (2011). Subaqueous morphology of Lake Lucerne (Central Switzerland): implications for mass movements and glacial history. *Swiss journal of geosciences*, *104*(3), 425-443.

Howarth, J. D., Fitzsimons, S. J., Norris, R. J., & Jacobsen, G. E. (2014). Lake sediments record high intensity shaking that provides insight into the location and rupture length of large earthquakes on the Alpine Fault, New Zealand. Earth and Planetary Science Letters, 403, 340-351.

Ito, M. (2008). Downfan transformation from turbidity currents to debris flows at a channel-to-lobe transitional zone: the lower Pleistocene Otadai Formation, Boso Peninsula, Japan. *Journal of Sedimentary Research*, *78*(10), 668-682.

Karlin, R. E., Holmes, M., Abella, S. E. B., & Sylwester, R. (2004). Holocene landslides and a 3500-year record of Pacific Northwest earthquakes from sediments in Lake Washington. *GSA Bulletin*, *116*(1-2), 94-108.

Kelts, K., & Hsü, K. J. (1980). Resedimented facies of 1875 Horgen slumps in Lake Zurich and a process model of longitudinal transport of turbidity currents. *Eclogae Geologicae Helvetiae*, *73*(1), 271-281.

Kremer, K., Hilbe, M., Simpson, G., Decrouy, L., Wildi, W., & Girardclos, S. (2015). Reconstructing 4000 years of mass movement and tsunami history in a deep peri-Alpine lake (Lake Geneva, France-Switzerland). *Sedimentology*, *62*(5), 1305-1327.

Kremer, K., Wirth, S. B., Reusch, A., Fäh, D., Bellwald, B., Anselmetti, F. S., ... & Strasser, M. (2017). Lake-sediment based paleoseismology: Limitations and perspectives from the Swiss Alps. Quaternary science reviews, 168, 1-18.

Lamarche, G., Mountjoy, J., Bull, S., Hubble, T., Krastel, S., Lane, E., ... & Woelz, S. (Eds.). (2016). *Submarine Mass Movements and Their Consequences: 7th International Symposium* (Vol. 41). Springer.

Lauterbach, S., Chapron, E., Brauer, A., Hüls, M., Gilli, A., Arnaud, F., ... & Participants, D. (2012). A sedimentary record of Holocene surface runoff events and earthquake activity from Lake Iseo (Southern Alps, Italy). *The Holocene*, *22*(7), 749-760.

Leithold, E. L., Wegmann, K. W., Bohnenstiehl, D. R., Smith, S. G., Noren, A., & O'Grady, R. (2018). Slope failures within and upstream of Lake Quinault, Washington, as uneven responses to Holocene earthquakes along the Cascadia subduction zone. *Quaternary Research*, *89*(1), 178-200.

Lindhorst, K., Gruen, M., Krastel, S., & Schwenk, T. (2012). Hydroacoustic analysis of mass wasting deposits in Lake Ohrid (FYR Macedonia/Albania). In *Submarine Mass Movements and Their Consequences* (pp. 245-253). Springer, Dordrecht.

Lindhorst, K., Krastel, S., Papenberg, C., & Heidarzadeh, M. (2014). Modeling submarine landslide-generated waves in Lake Ohrid, Macedonia/Albania. In *Submarine Mass Movements and Their Consequences* (pp. 497-506). Springer, Cham.

Lindhorst, K., Krastel, S., Reicherter, K., Stipp, M., Wagner, B., & Schwenk, T. (2015). Sedimentary and tectonic evolution of Lake Ohrid (Macedonia/Albania). *Basin Research*, *27*(1), 84-101.

Locat, J., & Lee, H. J. (2002). Submarine landslides: advances and challenges. *Canadian Geotechnical Journal*, *39*(1), 193-212.

Lowag, J., Bull, J. M., Vardy, M. E., Miller, H., & Pinson, L. J. W. (2012). High-resolution seismic imaging of a Younger Dryas and Holocene mass movement complex in glacial lake Windermere, UK. *Geomorphology*, *171*, 42-57.

Masson, D. G., Harbitz, C. B., Wynn, R. B., Pedersen, G., & Løvholt, F. (2006). Submarine landslides: processes, triggers and hazard prediction. *Philosophical Transactions of the Royal Society of London A: Mathematical, Physical and Engineering Sciences*, *364*(1845), 2009-2039.

Moernaut, J. (2010). *Sublacustrine landslide processes and their paleoseismological significance: revealing the recurrence rate of giant earthquakes in South-Central Chile* (Doctoral dissertation, Ghent University).

Moernaut, J., & De Batist, M. (2011). Frontal emplacement and mobility of sublacustrine landslides: results from morphometric and seismostratigraphic analysis. *Marine Geology*, *285*(1-4), 29-45.

Moernaut, J., De Batist, M., Heirman, K., Van Daele, M., Pino, M., Brümmer, R., & Urrutia, R. (2009). Fluidization of buried mass-wasting deposits in lake sediments and its relevance for paleoseismology: results from a reflection seismic study of lakes Villarrica and Calafquén (South-Central Chile). *Sedimentary Geology*, *213*(3-4), 121-135.

Moernaut, J., Van Daele, M., Heirman, K., Fontijn, K., Strasser, M., Pino, M., ... & De Batist, M. (2014). Lacustrine turbidites as a tool for quantitative earthquake reconstruction: New evidence for a variable rupture mode in south central Chile. *Journal of Geophysical Research: Solid Earth*, *119*(3), 1607-1633.

Moernaut, J., Van Daele, M., Strasser, M., Clare, M. A., Heirman, K., Viel, M., ... & Urrutia, R. (2017). Lacustrine turbidites produced by surficial slope sediment remobilization: a mechanism for continuous and sensitive turbidite paleoseismic records. *Marine Geology*, *384*, 159-176.

Normandeau, A., Lamoureux, S. F., Lajeunesse, P., & Francus, P. (2016). Sediment dynamics in paired High Arctic lakes revealed from high-resolution swath bathymetry and acoustic stratigraphy surveys. *Journal of Geophysical Research: Earth Surface*, *121*(9), 1676-1696.

Praet, N., Moernaut, J., Van Daele, M., Boes, E., Haeussler, P. J., Strupler, M., ... & De Batist, M. (2017). Paleoseismic potential of sublacustrine landslide records in a high-seismicity setting (south-central Alaska). *Marine Geology*, *384*, 103-119.

Sauerbrey, M. A., Juschus, O., Gebhardt, A. C., Wennrich, V., Nowaczyk, N. R., & Melles, M. (2013). Mass movement deposits in the 3.6 Ma sediment record of Lake El'gygytgyn, Far East Russian Arctic. *Climate of the Past*, *9*(4), 1949-1967.

Schnellmann, M., Anselmetti, F. S., Giardini, D., & McKenzie, J. A. (2005). Mass movement-induced fold-and-thrust belt structures in unconsolidated sediments in Lake Lucerne (Switzerland). *Sedimentology*, *52*(2), 271-289.

Schnellmann, M., Anselmetti, F. S., Giardini, D., & Mckenzie, J. A. (2006). 15,000 Years of mass-movement history in Lake Lucerne: Implications for seismic and tsunami hazards. *Eclogae Geologicae Helvetiae*, *99*(3), 409-428.

Schnellmann, M., Anselmetti, F. S., Giardini, D., McKenzie, J. A., & Ward, S. N. (2002). Prehistoric earthquake history revealed by lacustrine slump deposits. *Geology*, *30*(12), 1131-1134.

Shanmugam, G., & Wang, Y. (2015). The landslide problem. *Journal of Palaeogeography*, *4*(2), 109-166.

Siegenthaler, C., & Sturm, M. (1991). Slump induced surges and sediment transport in Lake Uri, Switzerland. *Internationale Vereinigung für theoretische und angewandte Limnologie: Verhandlungen*, *24*(2), 955-958.

Simonneau, A., Chapron, E., Vannière, B., Wirth, S. B., Gilli, A., Di-Giovanni, C., ... & Magny, M. (2013). Mass-movement and flood-induced deposits in Lake Ledro, southern Alps, Italy: implications for Holocene palaeohydrology and natural hazards. *Climate of the Past*, *9*, 825-840.

Smith, S. B., Karlin, R. E., Kent, G. M., Seitz, G. G., & Driscoll, N. W. (2013). Holocene subaqueous paleoseismology of Lake Tahoe. *Bulletin*, *125*(5-6), 691-708.

Solovyeva, M. A., Starovoytov, A. V., Akhmanov, G. G., Khlystov, O. M., Khabuev, A. V., Tokarev, M. Y., & Chensky, D. A. (2016). The evolution of slump-induced destruction of Kukuy Griva slope (Lake Baikal) revealed on the base of the data of seismic and acoustic surveys. *Moscow University Geology Bulletin*, *71*(6), 416-428.

Strasser, M., & Anselmetti, F. (2008). Mass-movement event stratigraphy in Lake Zurich; a record of varying seismic and environmental impacts. *Beiträge zur Geologie der Schweiz, Geotechnische Serie*, *95*, 23-41.

Strasser, M., Anselmetti, F. S., Fäh, D., Giardini, D., & Schnellmann, M. (2006). Magnitudes and source areas of large prehistoric northern Alpine earthquakes revealed by slope failures in lakes. *Geology*, *34*(12), 1005-1008.

Strasser, M., Hilbe, M., & Anselmetti, F. S. (2011). Mapping basin-wide subaquatic slope failure susceptibility as a tool to assess regional seismic and tsunami hazards. *Marine Geophysical Research*, *32*(1-2), 331-347.

Strasser, M., Monecke, K., Schnellmann, M., & Anselmetti, F. S. (2013). Lake sediments as natural seismographs: A compiled record of Late Quaternary earthquakes in Central Switzerland and its implication for Alpine deformation. *Sedimentology*, *60*(1), 319-341.

Strupler, M. (2017). *Basin-Wide Assessment of the Earthquake-Triggered Landslide-and Tsunami Hazard* (Doctoral dissertation, ETH Zurich).

Strupler, M., Danciu, L., Hilbe, M., Kremer, K., Anselmetti, F. S., Strasser, M., & Wiemer, S. (2018a). A subaqueous hazard map for earthquake-triggered landslides in Lake Zurich, Switzerland. *Natural Hazards*, *90*(1), 51-78.

Strupler, M., Hilbe, M., Kremer, K., Danciu, L., Anselmetti, F. S., Strasser, M., & Wiemer, S. (2018b). Subaqueous landslide-triggered tsunami hazard for Lake Zurich, Switzerland. *Swiss Journal of Geosciences*, 1-19.

Strupler, M., Hilbe, M., Anselmetti, F. S., Kopf, A. J., Fleischmann, T., & Strasser, M. (2017). Probabilistic stability evaluation and seismic triggering scenarios of submerged slopes in Lake Zurich (Switzerland). *Geo-marine letters*, *37*(3), 241-258.

Talling, P. J. (2013). Hybrid submarine flows comprising turbidity current and cohesive debris flow: Deposits, theoretical and experimental analyses, and generalized models. *Geosphere*, *9*(3), 460-488.

Talling, P. J., Allin, J., Armitage, D. A., Arnott, R. W., Cartigny, M. J., Clare, M. A., ... & Hill, P. R. (2015). Key Future Directions For Research On Turbidity Currents and Their Deposits. *Journal of Sedimentary Research*, *85*(2), 153-169.

Van Daele, M., Moernaut, J., Doom, L., Boes, E., Fontijn, K., Heirman, K., ... & Brümmer, R. (2015). A comparison of the sedimentary records of the 1960 and 2010 great Chilean earthquakes in 17 lakes: Implications for quantitative lacustrine palaeoseismology. *Sedimentology*, *62*(5), 1466-1496.

Vogel, H., Russell, J. M., Cahyarini, S. Y., Bijaksana, S., Wattrus, N., Rethemeyer, J., & Melles, M. (2015). Depositional modes and lake-level variability at Lake Towuti, Indonesia, during the past~ 29 kyr BP. *Journal of paleolimnology*, *54*(4), 359-377.

Wagner, B., Francke, A., Sulpizio, R., Zanchetta, G., Lindhorst, K., Krastel, S., ... & Lushaj, B. (2012). Possible earthquake trigger for 6th century mass wasting deposit at Lake Ohrid (Macedonia/Albania).

Waldmann, N., Anselmetti, F. S., Ariztegui, D., Austin Jr, J. A., Pirouz, M., Moy, C. M., & Dunbar, R. (2011). Holocene mass-wasting events in Lago Fagnano, Tierra del Fuego (54° S): implications for paleoseismicity of the Magallanes-Fagnano transform fault. *Basin Research*, *23*(2), 171-190.

Wiemer, G., Moernaut, J., Stark, N., Kempf, P., De Batist, M., Pino, M., ... & Kopf, A. (2015). The role of sediment composition and behavior under dynamic loading conditions on slope failure initiation: a study of a subaqueous landslide in earthquake-prone South-Central Chile. *International Journal of Earth Sciences*, *104*(5), 1439-1457.